A Global Climatology of Single-Layer and Overlapped Clouds and their Optical Properties Developed Using a New Algorithm Applied to Terra/MODIS Data

F.-L. Chang and Z. Li
Earth System Science Interdisciplinary Center
University of Maryland
College Park, Maryland

Z. Li
Department of Meteorology
University of Maryland
College Park, Maryland

Introduction

To date, weather satellites are the only tool to measure cloud and climate variables on a global scale, an objective addressed by the International Satellite Cloud Climatology Project (ISCCP) (Rossow and Schiffer 1991; Rossow and Schiffer 1999). However, there is a dearth of information concerning the global climatology of cloud vertical structure and cirrus cloud properties. This is because the often-used visible and infrared measurements made by weather satellites are overwhelmingly affected by thick water clouds. Thin cirrus clouds have a signal that is so faint that they are difficult to detect. This makes it problematic to retrieve the properties of cloud optical depth and cloud-top height for either of the overlapped cloud layers. Although high-altitude cirrus clouds are often very thin, their presence can bungle the retrieval of lower thick clouds, leading to large errors in the retrieval of cloud height and optical properties, as demonstrated in this paper and in Chang and Li (2004).

The unprecedented moderate-resolution imaging spectroradiometer (MODIS) provides imager data at a high spatial resolution (250-m to 1-km nadir resolution, depending on wavelengths) and a high spectral resolution at 36 bands (0.415 μm to 14.235 μm) (King et al. 2003). The cloud-top data available from the MODIS standard product provide much better information on cirrus cloud-top height. However, there is no information on the existence is of any lower clouds beneath the cirrus clouds, and, thus, no appropriation is made to separate the total column-integrated cloud optical depth in terms of high and low clouds. This is because the retrieval assumes a single-layer cloud.

In this study, we applied a new retrieval method developed by Chang and Li (2004) to one year of MODIS data for obtaining the climatologies of (1) single-layer water and ice clouds and two-layer cirrus overlapping water clouds and (2) the cloud-top altitudes and optical depths of the identified cloud types and the emissivity of semitransparent clouds. They are retrieved from the MODIS 1-km calibrated visible and infrared radiance data, the MODIS cloud mask product (Ackerman et al. 1998), and the cloud-top pressure/temperature derived from the CO_2-slicing method (Menzel et al. 2002). We will

classify clouds into different categories based on cloud-top pressure (Pc), visible optical depth (τ_{VIS}), and 11-μm high-cloud emissivity (ε_{hc}), and overlapping information.

The Overlapped Retrieval Algorithm

We developed an algorithm that detects the overlapped clouds and retrieves their optical properties. Details of the retrieval algorithm are given in Chang and Li (2004). The algorithm first determines the altitude of the high clouds based on the MODIS CO_2-slicing-derived Pc. An overlapped or non-overlapped situation is determined only when Pc <500 mb and ε_{hc} <0.85 (τ_{VIS} < ~4) using combined data from the CO_2 slicing channel and 11 μm channel. An automated retrieval procedure determines whether a high-cloud pixel contains single-layer or overlapped high clouds. When an overlapped low cloud is detected, its altitude is inferred from the average cloud-top altitude of the low clouds identified from the neighboring pixels.

The retrieval algorithm is implemented through lookup tables to accelerate the processing of large volumes of data. They were obtained following extensive radiative transfer simulations in the visible and IR channels for a two-layer cloud system (cirrus above water cloud). The ice-cloud layer adopts a fixed effective radius of r_e = 30 μm and uses the scattering phase functions of the fractal ice polycrystals. This follows the ISCCP ice cloud model (Rossow and Schiffer 1999), which has proven to be more favorable based on comparisons with observational data (Minnis et al. 1993b, Francis 1995, Descloitres et al. 1998). In particular, Descloitres et al. (1998) show that the observed angular distributions of the visible reflectances from cirrus clouds agree within a few percent with the calculations based on the fractal-polycrystal scattering phase functions. Liquid water cloud layers have a fixed effective radius of r_e = 10 μm, also following the ISCCP model, and Mie scattering phase functions are used for the water droplets.

The MODIS Data

The MODIS data used in this study are from the 5-km overcast scenes observed in January, April, July, and October 2001 by the Terra satellite (nominal overpass time 10:30am). The data have a near-global coverage and excludes the polar winter regions. The data are sampled every fourth day, so 8 days (day 2, 6, 10, 14, 18, 22, 26, and 30) are sampled from each month. Note that the Terra/MODIS instrument failed between mid-June and July 2, 2001, so the July 4 data were sampled to replace the July 2 data. Use of the sampled data instead of daily data is necessary to reduce the data volume and in consideration of sample independence in light of the life cycle of a cloud system. Analyses of these sampled data should provide reasonable global cloud characteristics because synoptic weather systems transit on a time scale of approximately 4 to 7 days, except for a potential bias due to the diurnal variation of cloud.

From our retrieval scheme, all of the 5-km overcast scenes are classified into five cloud categories (Chang and Li 2004), (1) High1: single-layer high thin clouds (cirrus, Pc <500 mb and ε_{hc} <0.85), (2) High2: high thin cloud overlapped with low clouds (Pc <500 mb and ε_{hc} 0.85), (3) High3: high thick clouds (Pc <500 mb and ε_{hc} >0.85, overlapping is undecided),(4) Low1: low clouds with no cirrus above (Pc >600 mb, assumed single-layer), and (5) Mid: middle clouds (500 mb ≤ Pc ≤ 600 mb, overlapping is undecided). The overlapped or non-overlapped situations are only determined for

Pc <500 mb, thus all Mid and Low1 clouds are undecided. For high clouds, they are only determined if ε_{hc} <0.85, which essentially represents cirrus clouds (Sassen et al. 2002). Thus, High3 are also undecided. The Mid cloud in this study is only an ad hoc definition used to separate the high and low clouds. Therefore, some Mid clouds may be overlapped with cirrus clouds or low clouds, but the percentage of such occurrences should be small, as revealed in this study.

Figure 1 shows the latitudinal distributions of the zonal-mean cloud amounts for the five cloud categories. The overall mean values for the five cloud categories are also calculated for each of the four months and are given in Table 1 in terms of the absolute cloud amount (upper rows) and relative percentage out of all 5-km overcast amounts (lower rows). Overall, the two most dominant cloud configurations are single-layer low and cirrus overlapping with low clouds. The latter accounts for about 30% of all overcast cases or 50% of all high clouds. It is the most frequently observed multilayer clouds that occur in nature, according to lidar measurements (D. Winker, private communication). The 30% does not include the 4% of extra overlapping clouds that were not processed because of a lack of single-layer low clouds nearby; so the true frequency is slightly higher. High clouds occurred most

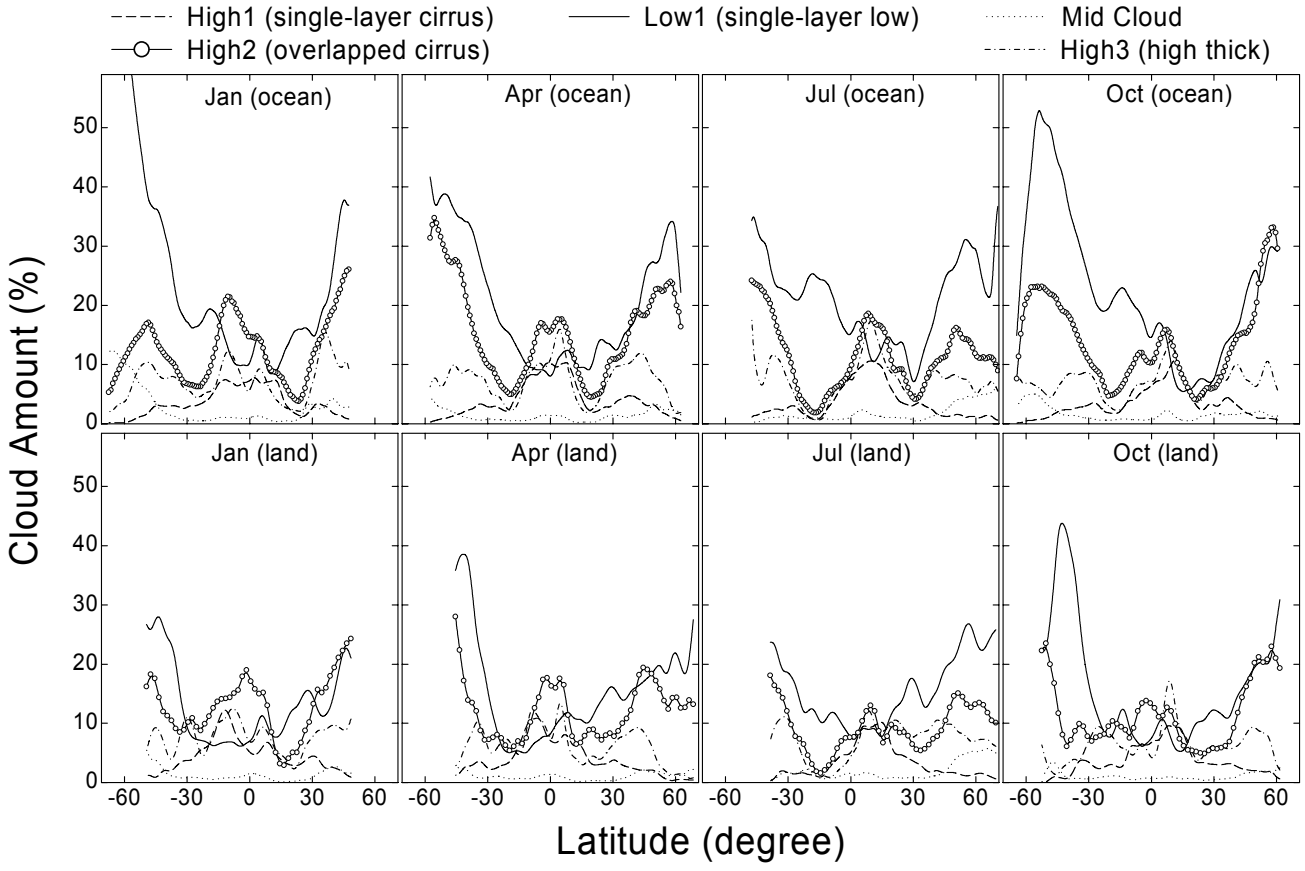

Figure 1. Zonal-mean frequency distributions of cloud amounts obtained for five cloud categories of High1, High2, High3, Mid, and Low1. Results are plotted separately for each month and over ocean and land.

Table 1. Absolute and relative frequencies of occurrence of High1, High2, High3, Mid, and Low1 clouds obtained for each month of January, April, July, and October 2001. Absolute frequencies (upper table) are computed as the percentage of occurrence out of all MODIS pixels and relative frequencies (lower table) are out of all 5-km overcast scenes. Results are given separately for ocean and land.

	Jan 2001	Apr 2001	Jul 2001	Oct 2001	Mean
Absolute (%)					
High1	4.3/5.5	4.6/4.8	3.4/3.7	4.0/5.2	4.1/4.8
High2	12.3/14.0	14.3/12.6	9.9/9.0	12.8/12.7	12.3/12.1
High3	7.6/9.3	7.9/7.6	7.2/7.6	7.9/9.1	7.6/8.4
Mid	2.3/1.4	1.2/1.0	1.8/2.2	1.5/1.1	1.7/1.4
Low1	22.4/13.6	18.8/14.0	20.4/16.2	20.6/14.5	20.6/14.6
Relative (%)					
High1	8.8/12.5	9.9/11.9	7.9/9.5	8.6/12.2	8.8/11.5
High2	25.2/32.0	30.5/31.5	23.3/23.4	27.2/29.8	26.6/29.2
High3	15.6/21.2	16.9/18.9	16.8/19.6	16.9/21.3	16.6/20.2
Mid	4.6/3.2	2.6/2.6	4.3/5.6	3.3/2.6	3.7/3.5
Low1	45.8/31.1	40.1/35.1	47.7/42.0	44.0/34.1	44.4/35.6

frequently over the ITCZ and midlatitudes and are seldom in the subtropics. Tropical high clouds are associated with extensive anvil cirrus clouds covering large spatial domains. In higher latitudes, they are accompanied by storms and fronts, as revealed from ground observations (Warren et al. 1985). The optically thick high clouds (High3) with ε_{hc} >0.85 are also more frequent in the tropics due to deep convection and over mid-latitudes due to mesoscale cyclones. Even though their absolute cloud amounts are similar, relatively more high clouds are found over land than over ocean. There are fewer low clouds (Low1) than total high clouds (High1+High2+High3), especially over land. This is partially because the satellite views from above so high clouds may obscure lower clouds. So in regions of prevailing high clouds, low clouds would be missed that we attempt to "recover" for the frequently occurring cirrus over water clouds.

A Bimodal Distribution of Cloud Vertical Structure

Figure 2 shows the monthly frequency distributions of Pc. To better visually display the vertical structure of all clouds, the curves representing different categories are recombined. For example, the same curve is used for single-layer low, mid-level, and high clouds because their altitudes are indicated by Pc itself. On the other hand, an overlapped low cloud (Low2) is added that has the same total frequency of occurrence as High2. Of course, Low2 and High2 are from the same overlapped clouds, but they differentiate the higher and lower portions. The total frequencies of all cloud types are also plotted.

From the figure, a distinct bimodal Pc distribution is seen with a universal minimum at around 530 mb in each sub-panel and two maxima at around 275 mb and around 725 mb. When including all MODIS-retrieved Pc, i.e., not limited to the 5-km overcast pixels, we found less than 4% of clouds having their tops falling between 500 mb and 600 mb. The bimodal Pc distribution corresponds to two typical cloud

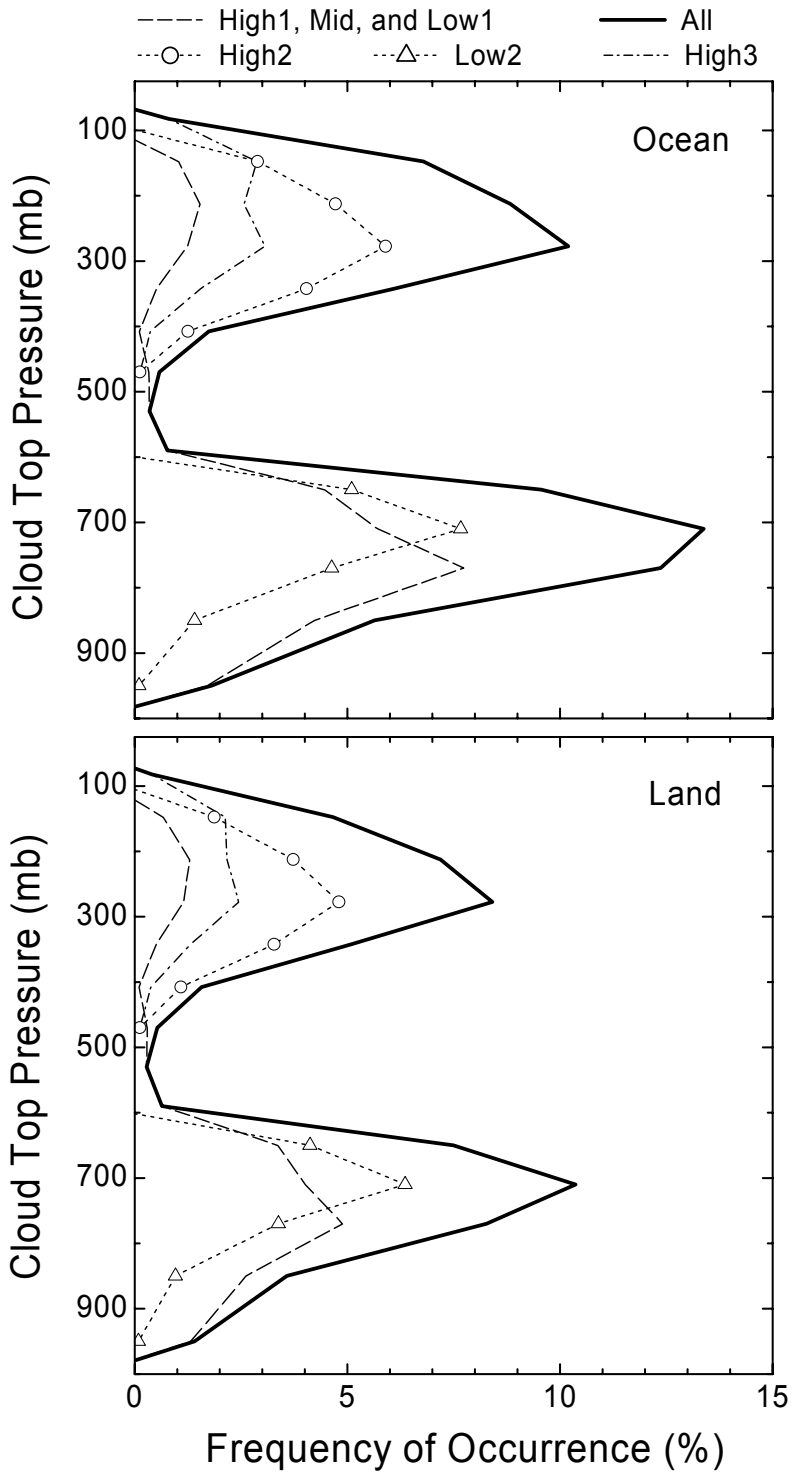

Figure 2. Frequency distributions of Pc obtained for the six cloud categories of High1, High2, High3, Mid, Low1, and Low2. Results are obtained for April 2001 and shown separately for over ocean and land. Note that the frequencies of High1, Low1, and Mid are connected as one line and the total frequency for all clouds is plotted in thick solid lines.

systems: (1) dominant low-level stratiform clouds, like shallow cumulus and stratocumulus, which are often organized into cloud bands and patches (Kuettner 1971; Agee 1984); and (2) high clouds resulting from synoptic weather systems, like midlatitude fronts, cyclones, and tropical storms, which are often organized into large-scale patterns of cirrus clouds, squall lines, and deep convective clouds (Starr and Cox 1985; Sheu et al. 1997). Note that the two-layer pattern is not a direct consequence of using the two-layer retrieval algorithm, as a cloud top may be located anywhere. It is true, however, that the algorithm cannot retrieve more than two layers of cloud and, thus, the retrieved low clouds may represent the average of all multilayer low clouds beneath the cirrus, as identified from the neighboring pixels. There is no hope to resolve multi-layer low clouds, unless ground-based or space-borne radar are used (Mace et al. 2001, Stephens et al. 2002). Fortunately, high thin cirrus over water clouds occur much more frequently than multilayer low clouds (Winker, private communication).

The overall frequencies of occurrence of the 5-km overcast Pc and τ_{VIS} from the four-month near-global dataset over ocean and land are shown in Figure 3. The upper panels represent the MODIS standard product that applies the single-layer cloud retrieval model and the lower panels from the overlapped retrievals. Both the Pc and τ_{VIS} intervals follow the ISCCP (Rossow and Schiffer 1991), where Pc intervals are at 1000-900 mb, 900-800 mb, 800-740 mb, 740-680 mb, 680-620 mb, 620-560 mb, 560-500 mb, 500-440 mb, 440-375 mb, 375-310 mb, 310-225 mb, 225-180 mb, 180-115 mb, and 115-50 mb. The numbers in each panel indicate the total cloud amounts obtained over ocean (left sub-panel), over land (right sub-panel), and are given separately for Pc <530 mb and Pc ≥530 mb. It should be emphasized that the MODIS only provides the height of the very top layer of a cloud. Through our retrieval, approximately 12% (absolute frequency of occurrence or about 27% and 29% relative values) of the clouds of high tops were determined to contain low clouds that overlap with high cirrus clouds. If one uses the MODIS cloud-top data alone to determine the fractions of high and low clouds, the latter would be substantially underestimated.

Likewise, the MODIS τ_{VIS} retrievals do not differentiate high and low clouds, except for providing a single cloud-top height. Apparently, attributing the retrieved τ_{VIS} to the cloud, as designated by the MODIS cloud top, would significantly overestimate τ_{VIS} for true high-clouds whose optical depths should be much less than lower water clouds. The values of τ_{VIS} for the high clouds, as seen in Figure 3a, are actually the sum of both high and low clouds. This is confirmed with a preliminary comparison against the Atmospheric Radiation Measurement (ARM) ground-based radar observations of cloud vertical structure (Chang and Li 2004). Another bias arises in choosing a cloud model for retrieving τ_{VIS} for the two-layered ice-over-water clouds. Regarding such overlapped clouds as single-layer clouds, use of either a water or ice cloud model can lead to significant biases.

Figure 4 shows the variations of zonal-mean Pc (Figure 4a), Tc (Figure 4b), and τ_{VIS} (Figure 4c) corresponding to each of the six cloud categories. From Figure 4a, Pc for the High1, High2, and High3 clouds changes the most between 200–400 mb; it is highest (~200 mb) in the tropics and lowers toward higher latitudes. Pc for Low1 and Low2 clouds varies mostly between 680–800 mb with a much weaker latitudinal variability. From Figure 4b, the high clouds are found mostly between 215–245 K with the lowest Tc in the tropics (~215K). For the low-clouds with similar Pc, their Tc decreases from approximately 285 K in the tropics to less than 270 K at higher latitudes, a trend similar to surface temperature.

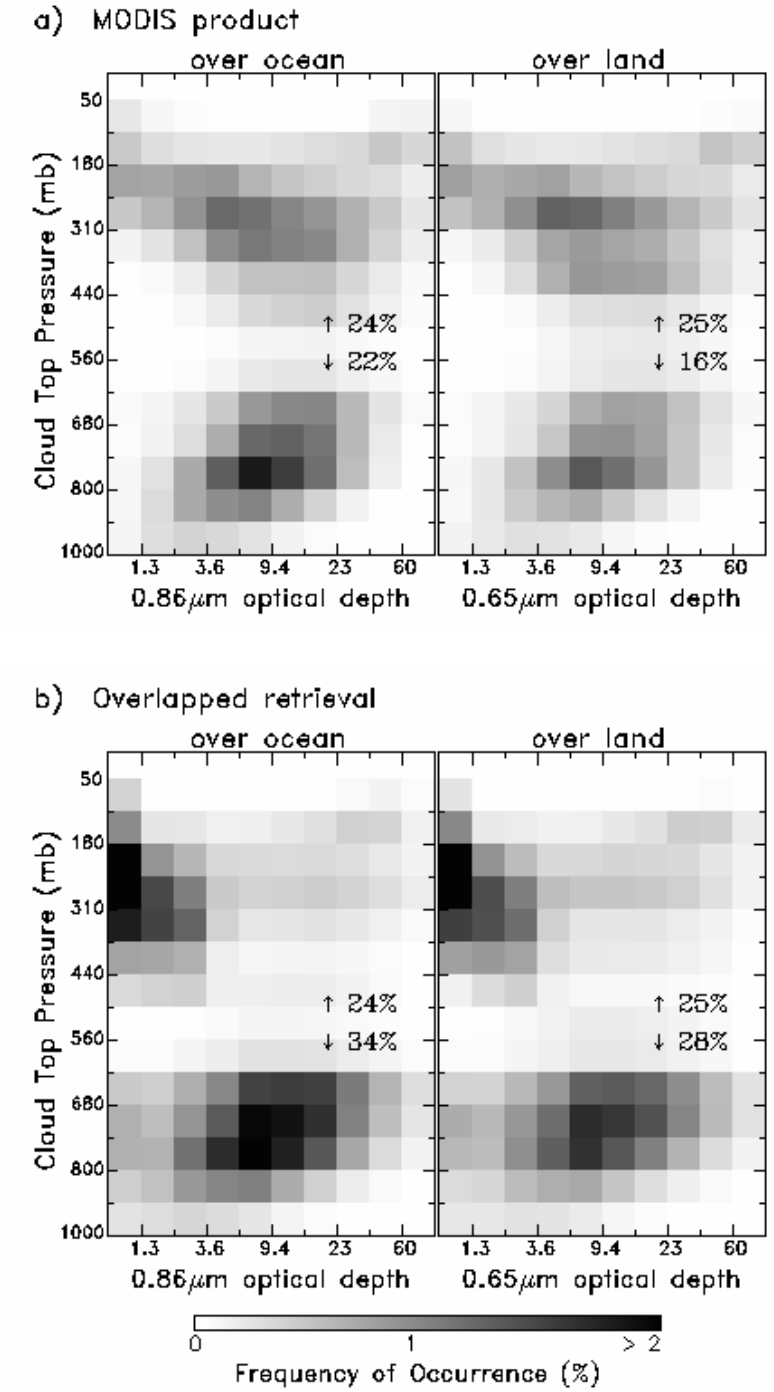

Figure 3. Frequencies of occurrence of the 5-km overcast Pc and τ_{VIS} obtained from the four-month near-global dataset for a) the MODIS standard product and b) the overlapped retrievals. Results are shown separately for over ocean (left sub-panel) and land (right sub-panel). The numbers in each sub-panel indicated the total percentages of Pc above (↑) and below (↓) 530 mb.

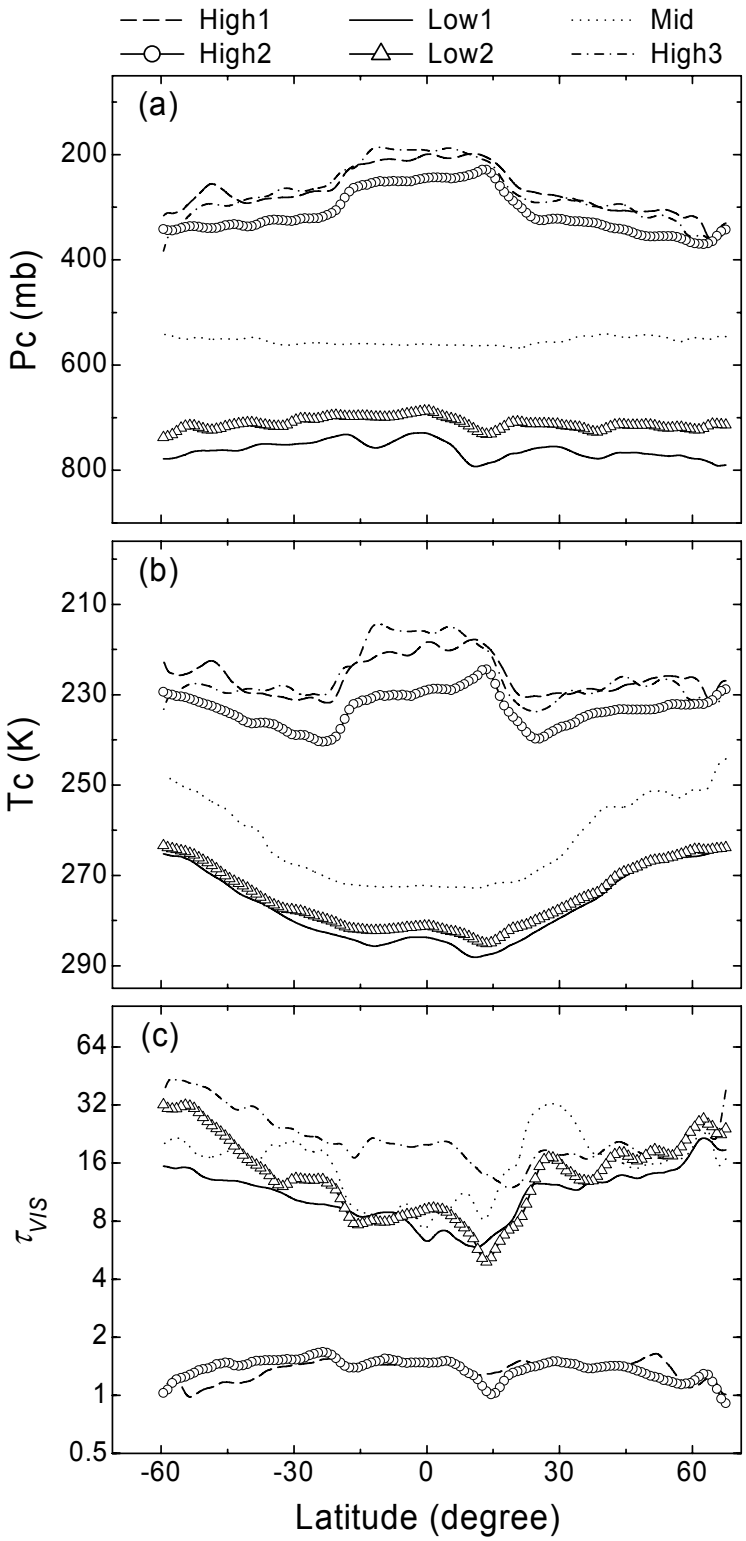

Figure 4. Latitudinal distributions of the zonal-mean Pc (a), Tc (b), and τ_{VIS} (c) obtained for the six cloud categories of High1, High2, High3, Mid, Low1, and Low2. Results show for April 2001.

Differences in Tc (Pc) between the high clouds and the low clouds are thus largest in the tropics and smallest at higher latitudes. Some dips in the Pc and Tc around 15° to 30° in both hemispheres are attributed to the subtropical subsidence regions. The Mid cloud Pc and Tc are also plotted in the figures for reference.

Comparisons with the MODIS Standard Products

In our retrievals, τ_{VIS} for cirrus clouds, single-layered (High1), and overlapped (High2), was estimated through an infrared radiative transfer scheme. It is unlike the standard MODIS retrieval algorithm that uses reflectance measurements for cirrus retrieval, which has more bearing on the uncertainty of the ice-crystal scattering phase functions. Figure 5 shows an example of the latitudinal distributions of τ_{VIS} obtained from the MODIS standard product for the cloud categories of High1, High2, High3, Mid, and Low1. The figure shows April only, but the patterns of January, July, and October are similar. The monthly mean MODIS τ_{VIS} obtained for the five cloud categories are given in Table 3. In comparison to the same case but obtained from our algorithm, as is shown in Figure 4c, the latitudinal distributions of τ_{VIS} are very similar, except for the large differences for overlapped clouds that were separated by our algorithm, but not by the MODIS.

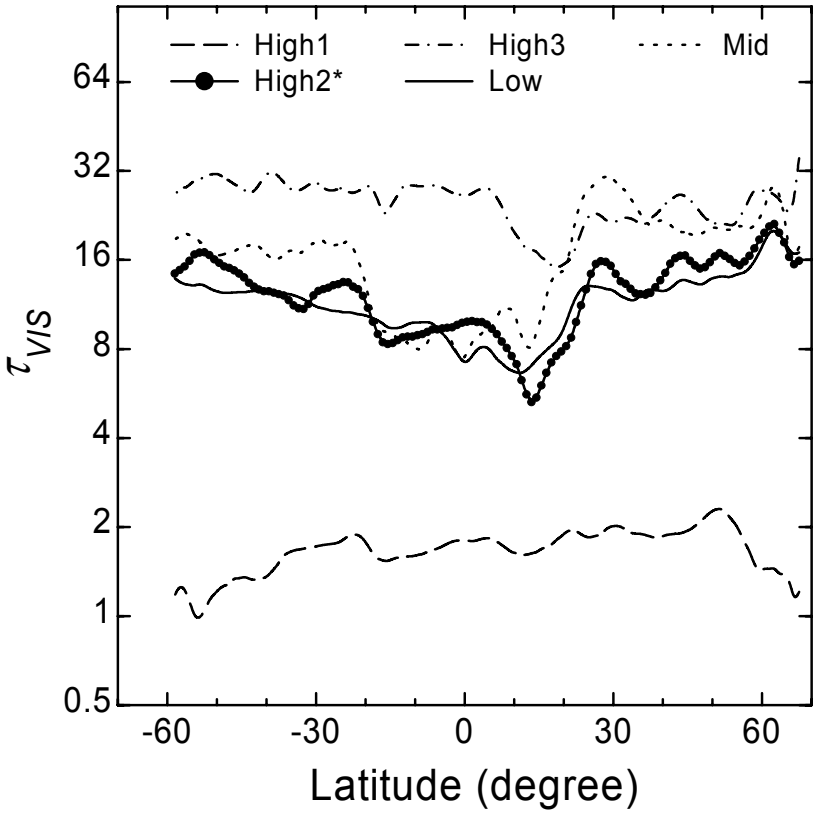

Figure 5. Latitudinal distributions of zonal-mean τ_{VIS} obtained from the MODIS standard products for April 2001. Note that High2* is from the MODIS single-layered retrieval, so there is no Low2.

Figure 6 shows the latitudinal distributions of zonal-mean ε_{hc} (April only) obtained for the High1, High2, and High3 cloud categories. The High1 and High3 ε_{hc} from our retrievals are the same as from the MODIS standard products. However, High2 ε_{hc} (lines with open points) are from our retrievals whereas High2* ε_{hc} (lines with solid points) are from the MODIS products. These two different ε_{hc} were both calculated using Eq. (2) except that the calculations of High2* assume that $R'(\upsilon) = R_{clr}(\upsilon)$ without accounting for the low-cloud effect. The corresponding global mean ε_{hc} for all the months are given in Table 2 for High1, High2, and High3 clouds and in Table 3 for High2* clouds. As seen from the figure and tables, the single-layer cirrus (High1) and the overlapped cirrus (High2) both have similar mean ε_{hc} with differences less than ±0.01-0.02. However, if no correction is made to account for the overlapping effect, as in the case of High2*, the mean ε_{hc} can be significantly overestimated by a magnitude of ~0.10. This difference in ε_{hc} (20% relative) leads to an overestimate in τ_{VIS} of ~0.5, or 30% of the mean τ_{VIS}.

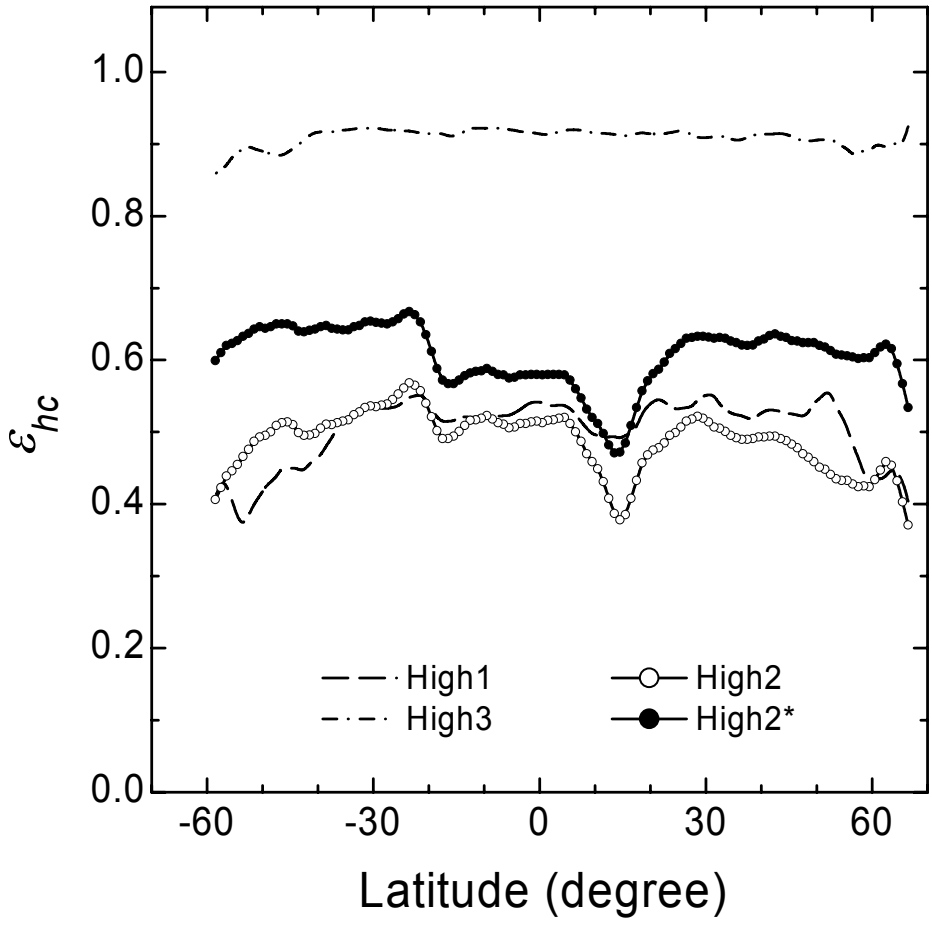

Figure 6. Latitudinal distributions of the zonal-mean ε_{hc} obtained for High1, High2, and High3 cloud categories and for High2* from the MODIS standard product. Results are plotted for April 2001.

Table 2. Mean Pc, Tc, and τ_{VIS} for High1, High2, High3, Mid, Low1, and Low2 cloud categories and mean ε_{hc} for High1, High2, and High3. The means are given separately for ocean/land in each month. The overall mean of the 4 months is also given in last column.

	January 2001	April 2001	July 2001	October 2001	Mean
Pc (mb)					
High1	285/253	262/263	289/293	283/262	280/268
High2	322/292	307/300	322/324	320/302	318/304
High3	285/252	265/261	276/280	271/254	274/262
Mid	556/558	555/558	556/557	555/558	556/558
Low1	757/759	762/754	762/756	758/763	760/758
Low2	705/705	712/706	706/700	707/708	708/705
Tc (K)					
High1	229/225	226/226	233/234	230/228	230/228
High2	236/232	234/233	238/240	236/235	236/235
High3	229/224	226/225	230/231	227/226	228/227
Mid	264/267	264/265	267/268	264/266	265/267
Low1	278/280	278/278	280/281	278/280	279/280
Low2	276/277	276/276	278/278	276/278	277/277
τ_{VIS}					
High1	1.45/1.38	1.35/1.39	1.51/1.57	1.40/1.41	1.43/1.44
High2	1.60/1.47	1.40/1.40	1.63/1.67	1.55/1.54	1.54/1.52
High3	21.1/21.2	22.4/19.0	23.1/22.3	22.6/21.4	22.3/21.0
Mid	15.9/13.8	16.5/14.8	17.5/17.0	17.9/15.2	17.0/15.2
Low1	10.8/10.1	10.7/10.6	10.4/10.8	11.1/10.6	10.8/10.5
Low2	13.3/12.2	14.3/12.6	13.8/13.9	14.0/13.4	13.8/13.0
ε_{hc}					
High1	0.52/0.51	0.50/0.51	0.54/0.55	0.51/0.52	0.52/0.52
High2	0.54/0.51	0.49/0.49	0.55/0.56	0.53/0.53	0.53/0.52
High3	0.92/0.91	0.91/0.91	0.92/0.92	0.92/0.92	0.92/0.92

Table 3. Mean τ_{VIS} for High1, High2*, High3, Mid, and Low1 and mean ε_{hc} for High2* as obtained from the MODIS standard retrieval products. The High2* is assuming single-layer cloud with no presence of low clouds. The means are given in the format similar to those shown in Table 2.

	January 2001	April 2001	July 2001	October 2001	Mean
τ_{VIS}					
High1	1.69/1.65	1.65/1.73	1.77/1.89	1.65/1.73	1.69/1.75
High2	12.5/10.8	12.3/11.9	12.6/13.2	12.8/11.9	12.6/12.0
High3	25.9/24.8	25.4/24.5	27.1/27.4	26.9/25.3	26.3/25.5
Mid	16.1/13.5	16.8/15.4	17.1/16.5	18.0/15.0	17.0/15.1
Low1	11.2/10.5	11.0/11.1	10.8/11.4	11.3/10.9	11.1/11.0
ε_{hc}					
High2	0.64/0.61	0.61/0.60	0.64/0.65	0.64/0.62	0.63/0.62

Concluding Remarks

Of all 5-km overcast scenes that are processed in this study, the following temporal frequencies of occurrence were obtained. The results are separated over ocean and land with the frequencies over land given in parentheses: 52% (61%) for high clouds with Pc <500 mb, ~35% (~41%) for high cirrus clouds with ε_{hc} <0.85, 27% (~29%) for high cirrus clouds overlapped with low clouds, ~71% (65) for low clouds having Pc >600 mb, in which ~44% (36%) for single-layer low clouds. The remaining middle clouds with a cloud-top altitude between 500–600 mb occurred less than 4% over both ocean and land. The retrieved cirrus clouds have a mean value of τ_{VIS} ~1.5 and ε_{hc} ~0.5, which are very similar for both the single-layer and overlapped cirrus clouds.

The majority of cloud-top heights occur in two distinct layers, one in the upper troposphere and one in the lower troposphere. The former has a maximum at around 275 mb and the latter has a maximum at around 725 mb. It is a ubiquitous phenomenon occurring at almost all latitudes and in all seasons. In between is a distinct region of extremely low occurrence (<4%) of cloud tops between 500 mb and 600 mb. This characteristic may shed light on understanding cloud dynamical and radiative processes for improving cloud and climate modelling. Note, these results do not result from the use of our two-layer retrieval model, as the model can identify and retrieve both single- and two-layers clouds at any altitude. However, multilayer clouds below thick high clouds could be missed by this and any other method.

As the MODIS products only provide one cloud top for both single-layer and overlapped clouds, use of these cloud-top data would underestimate the low clouds by 30% that overlap with high cirrus clouds whose optical depths would be overestimated by a factor of about 7. In comparison with the ISCCP global cloud climatology presented in Zhang et al. (2004), large discrepancies also exist. ISCCP has much more middle cloud and less high and low clouds; therefore, ISCCP does not show a distinct two-layer cloud structure. More detailed comparisons will be conducted and presented in the future.

In light of such substantial differences in the cloud vertical structure that result simply from different inversion algorithms, much caution is warranted in validating general circulation models and improving their cloud parameterization schemes. At present, results of cloud simulations from many general circulation models have been validated against ISCCP total cloud amounts, promoting many improvements in the models. There is increasing attention on more detailed comparisons that concern the vertical distribution of clouds. For example, the current ARM Cloud Parameterization and Modelling (ARMCPM) working group have collected and analyzed 10 sets of general circulation model-simulated cloud layer data and compared them to the statistics of the ISCCP (Zhang et al. 2004). It was found that most general circulation models produce substantially less middle and low clouds than the ISCCP. In general, compared to that of the ISCCP, the general circulation models' mid-level cloud amounts are closer to our new retrieval products, whereas the general circulation models' low cloud amounts are even further away from our retrievals. Clearly, it is very critical to sort out these differences to improve the performance of general circulation models and other types of models of better resolution.

Acknowledgements

This research would not have been possible without the dedicated work of the MODIS Atmospheres Team in processing the cloud mask and cloud properties. The authors are grateful to the National Aeronautics and Space Administration (NASA) Goddard Earth Sciences Distributed Active Archived Center for providing the MODIS data. Funding for this work was supported by the DOE Grant No. DE-FG02-01ER63166 under the Atmospheric Radiation Measurement Program and NASA Grant No. NNG04GE79G.

Corresponding Author

Dr. Fu-Lung Chang, fchang@essic.umd.edu, (301) 405-5568

References

Ackerman, S. A., K. I. Strabala, W. P. Menzel, R. A. Frey, C. C. Moeller, and L. E. Gumley, 1998: Discriminating clear-sky from clouds with MODIS. *J. Geophys. Res.*, **103**, 32,141-32,158.

Agee, E. M., 1984: Observations from space and thermal convection: A historical perspective. *Bull. Amer. Meteor. Soc.*, **65**, 938-949.

Chang, F.-L., and Z. Li, 2004: Detecting cirrus-overlapping-water clouds and retrieving their optical properties using MODIS data. *J. Atmos. Sci.*, submitted.

Descloitres, J. C., J. C. Buriez, F. Parol, and Y. Fouquart, 1998: POLDER observations of cloud bidirectional reflectances compared to a plane-parallel model using the International Satellite Cloud Climatology Project cloud phase functions. *J. Geophys. Res.*, **103**, 11,411-11,418.

Francis, P. N., 1995: Some aircraft observations of the scattering properties of ice crystals. *J. Atmos. Sci.*, **52**, 1142-1154.

King, M. D., W. P. Menzel, Y. J. Kaufman, D. Tanre, B. C. Gao, S. Platnick, S. A. Ackerman, L. A. Remer, R. Pincus, and P. A. Hubanks, 2003: Cloud and aerosol properties, precipitable water, and profiles of temperature and humidity from MODIS. *IEEE Trans. Geosci. Remote Sens.*, **41**, 442-458.

Kuettner, J. P., 1971: Cloud bands in the earth's atmosphere. *Tellus*, **23**, 404-425.

Mace, G. G., E. E. Clothiaux, T. A. Ackerman, 2001: The composite characteristics of cirrus clouds: Bulk properties revealed by one year of continuous cloud radar data. *J. Climate*, 1**4**, 2185-2203.

Menzel, W. P., B. A. Baum, K. I. Strabala, and R. A. Frey, 2002: Cloud top properties and cloud phase-Algorithm Theoretical Basis Document: ATBD-MOD-04, p. 61. Available at http://modis-atmos.gsfc.nasa.gov/_docs/atbd_mod04.pdf.

Minnis, P., P. W. Heck, and D. F. Young, 1993b: Inference of cirrus cloud properties using satellite-observed visible and infrared radiances. Part II: Verification of theoretical cirrus radiative properties. *J. Atmos. Sci.*, **50**, 1305-1322.

Rossow, W. B., and R. A. Schiffer, 1991: ISCCP cloud data products. *Bull. Amer. Meteor. Soc.*, **72**, 2-20.

Rossow, W. B., and R. A. Schiffer, 1999: Advances in understanding clouds from ISCCP. *Bull. Amer. Meteor. Soc.*, **80**, 2261-2287.

Sassen, K., Z. Wang, C. M. R. Platt, J. M. Comstock, 2002: Parameterization of infrared absorption in midlatitude cirrus clouds. *J. Atmos. Sci.*, 60, 428–433.

Sheu, R.-S., J. A. Curry, and G. Liu, 1997: Vertical stratification of tropical cloud properties as determined from satellite. *J. Geophys. Res.*, **102**, 4231-4245.

Starr, D. O'C., and S. K. Cox, 1985: Cirrus clouds. Part II: Numerical experiments on the formation and maintenance of cirrus. *J. Atmos. Sci.*, **42**, 2682-2694.

Stephens, G. L., and coauthors, 2002: The CLOUDSAT mission and the A-Train. *Bull. Amer. Meteor. Soc.*, **83**, 1771-1790.

Warren, S. G., C. J. Hahn, and J. London, 1985: Simultaneous occurrence of different cloud types. *J. Climate Appl. Meteor.*, **24**, 658-667.

Zhang, M. H., et al., 2004: Comparing clouds and their seasonal variations in 10 atmospheric general circulation models with satellite measurements, to be submitted to Special Issue of ARMCPM, *J. Geophys. Res.*.